

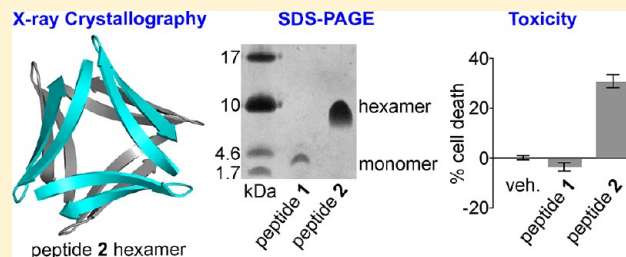
## A Hexamer of a Peptide Derived from $A\beta_{16-36}$

Adam G. Kreutzer, Ryan K. Spencer,<sup>1b</sup> Kate J. McKnelly, Stan Yoo, Imane L. Hamza, Patrick J. Salvesson, and James S. Nowick<sup>\*1b</sup>

Department of Chemistry, University of California, Irvine, Irvine, California 92697-2025, United States

### S Supporting Information

**ABSTRACT:** The absence of high-resolution structures of amyloid oligomers constitutes a major gap in our understanding of amyloid diseases. A growing body of evidence indicates that oligomers of the  $\beta$ -amyloid peptide  $A\beta$  are especially important in the progression of Alzheimer's disease. In many  $A\beta$  oligomers, the  $A\beta$  monomer components are thought to adopt a  $\beta$ -hairpin conformation. This paper describes the design and study of a macrocyclic  $\beta$ -hairpin peptide derived from  $A\beta_{16-36}$ . Sodium dodecyl sulfate–polyacrylamide gel electrophoresis and size exclusion chromatography studies show that the  $A\beta_{16-36}$   $\beta$ -hairpin peptide assembles in solution to form hexamers, trimers, and dimers. X-ray crystallography reveals that the peptide assembles to form a hexamer in the crystal state and that the hexamer is composed of dimers and trimers. Lactate dehydrogenase release assays show that the oligomers formed by the  $A\beta_{16-36}$   $\beta$ -hairpin peptide are toxic toward neuronally derived SH-SY5Y cells. Replica-exchange molecular dynamics demonstrates that the hexamer can accommodate full-length  $A\beta$ . These findings expand our understanding of the structure, solution-phase behavior, and biological activity of  $A\beta$  oligomers and may offer insights into the molecular basis of Alzheimer's disease.



Elucidating the structures of oligomers formed by amyloidogenic peptides and proteins represents a frontier in structural biology and constitutes a major challenge in understanding the molecular basis of amyloid diseases. The heterogeneity and metastability of amyloid oligomers hinder the isolation of homogeneous amyloid oligomers that are suitable for structural elucidation by nuclear magnetic resonance (NMR) spectroscopy and X-ray crystallography. More than 30 different amyloidogenic peptides and proteins have been identified, yet only a few high-resolution structures have shed light on amyloid oligomers thus far.

X-ray crystallographic studies of fragments of amyloidogenic peptides and proteins have provided insights into the structures of amyloid oligomers.<sup>1–4</sup> Eisenberg and co-workers determined the X-ray crystallographic structure of a  $\beta$ -barrel-like oligomer, termed a cylindrin, formed by an 11-residue peptide fragment from  $\alpha$ B crystallin.<sup>1</sup> The cylindrin oligomer is composed of six  $\beta$ -strands that form a twisted antiparallel  $\beta$ -sheet that closes back on itself to form a cylinder. Surewicz and co-workers determined the X-ray crystallographic structure of a hexameric oligomer formed by a disulfide-stabilized  $\beta$ -sheet fragment from human prion protein (hPrP).<sup>2</sup> The hPrP oligomer is composed of three four-stranded antiparallel  $\beta$ -sheets that pack to form a hydrophobic core. Our laboratory determined the X-ray crystallographic structure of a tetramer formed by a macrocyclic peptide containing a nine-residue fragment from  $\beta$ -amyloid peptide  $A\beta$ .<sup>4</sup> Although the peptide fragments in these three different studies vary in sequence, the three structures share common features of being discrete oligomers composed of antiparallel  $\beta$ -sheets that form packed hydrophobic cores.

Biological and solution-phase studies have revealed that oligomers formed by different amyloidogenic peptides and proteins share common biological and structural properties.<sup>5,6</sup> Amyloid oligomers are typically toxic toward cells, an important characteristic that is thought to play a role in the pathogenesis of amyloid diseases.<sup>1,7,8</sup> Amyloid oligomers are typically stable to sodium dodecyl sulfate (SDS), migrating as discrete assemblies in SDS–polyacrylamide gel electrophoresis (PAGE) experiments.<sup>9,10</sup> Amyloid oligomers appear to be composed of antiparallel  $\beta$ -sheets, while amyloid fibrils are generally composed of parallel  $\beta$ -sheets.<sup>11–16</sup> Furthermore, the monomer building blocks of many amyloid oligomers are thought to adopt the simplest arrangement of an antiparallel  $\beta$ -sheet, a  $\beta$ -hairpin.<sup>17–25</sup>

Our laboratory has determined the X-ray crystallographic structures of oligomers formed by macrocyclic  $\beta$ -sheet peptides designed to mimic  $\beta$ -hairpins from amyloidogenic peptides and proteins.<sup>26–30</sup> These  $\beta$ -hairpin peptides contain two heptapeptide  $\beta$ -strand fragments locked in an antiparallel  $\beta$ -sheet by two  $\delta$ -linked ornithine ( $\delta$ Orn) turn mimics and also contain an *N*-methyl group that blocks uncontrolled aggregation.<sup>31–33</sup> These design features permit crystallization of the  $\beta$ -hairpin peptides and structural elucidation of the higher-order oligomers they can form. The  $\beta$ -hairpin peptides have two surfaces: a major surface that displays eight of the 14 side chains and a minor surface that displays the six remaining side chains. **Figure 1**

Received: August 24, 2017

Revised: October 9, 2017

Published: October 13, 2017

shows a generic structure of these  $\beta$ -hairpin peptides and highlights the major and minor surfaces in red and blue.

To date, our laboratory has elucidated the X-ray crystallographic structures of oligomers formed by  $\beta$ -hairpin peptides derived from  $A\beta$ ,<sup>26–28,34</sup>  $\alpha$ -synuclein,<sup>29</sup> and  $\beta_2$ -microglobulin.<sup>30</sup> These structures revealed the propensity for  $\beta$ -hairpin peptides to form oligomers in the crystal state, including dimers, trimers, hexamers, octamers, nonamers, and dodecamers. The different oligomers identified in these studies demonstrate the diversity and polymorphism of the structures that different amyloid-derived  $\beta$ -hairpin peptides can form.

Previously, we reported the X-ray crystallographic structures of oligomers formed by  $\beta$ -hairpin peptide 1 (Figure 2A), which is derived from an  $A\beta_{17–36}$   $\beta$ -hairpin (Figure 2B).<sup>26,35</sup> Peptide 1 contains  $A\beta_{17–23}$  and  $A\beta_{30–36}$   $\beta$ -strands linked by two  $\delta$ Orn turn units; the  $\delta$ Orn turn that links Asp<sub>23</sub> and Ala<sub>30</sub> replaces the  $A\beta_{24–29}$  loop of the  $A\beta_{17–36}$   $\beta$ -hairpin. Peptide 1 also contains an *N*-methyl group on Phe<sub>20</sub> and an  $\alpha$ -linked ornithine at position 35 as a hydrophilic isostere of methionine. The X-ray crystallographic structure reveals that peptide 1 assembles hierarchically to form a triangular trimer that further assembles with a second triangular trimer to form a sandwichlike hexamer (Figure 3).<sup>36</sup>

In this study, we set out to explore how shifting registration by one amino acid toward the N-terminus affects the structural and biological properties of a  $\beta$ -hairpin peptide. Shifting the  $\beta$ -hairpin registration is significant, because it changes both the pairings of the residues within the  $\beta$ -hairpin and the surfaces upon which the side chains are displayed. In the  $A\beta_{17–36}$   $\beta$ -hairpin, from which peptide 1 is derived, Ile<sub>31</sub> pairs with Glu<sub>22</sub> in the shifted  $A\beta_{16–36}$   $\beta$ -hairpin, Ile<sub>31</sub> pairs with Ala<sub>21</sub>. In the  $A\beta_{17–36}$   $\beta$ -hairpin, the side chain of Glu<sub>22</sub> shares the same surface as the side chain of Ile<sub>31</sub>; in the  $A\beta_{16–36}$   $\beta$ -hairpin, the side chain of Glu<sub>22</sub> is on the opposite surface. We find that the resulting shifted  $\beta$ -hairpin peptide not only assembles in the crystal state to form oligomers but also exhibits both solution-phase assembly and toxicity reminiscent of amyloid oligomers.

Here we describe the X-ray crystallographic, solution-phase, and biological studies of peptide 2 (Figure 2C), which is designed to mimic the  $A\beta_{16–36}$   $\beta$ -hairpin (Figure 2D). Peptide 2 contains  $A\beta_{16–22}$  and  $A\beta_{30–36}$   $\beta$ -strands linked by two  $\delta$ Orn turn units, an *N*-methyl group on Phe<sub>19</sub>, and the native methionine residue at position 35. Peptide 2 runs as a hexamer in SDS-PAGE and appears to form dimers and trimers in size exclusion chromatography (SEC). The oligomers formed by peptide 2 are toxic toward human neuroblastoma cell line SH-SY5Y. X-

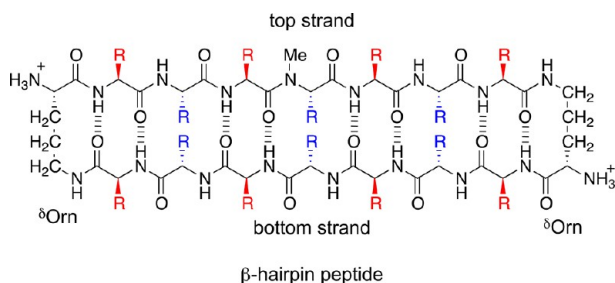


**Figure 1.** Generic chemical structure of a  $\beta$ -hairpin peptide. Two heptapeptide  $\beta$ -strands, a top strand and a bottom strand, are connected by two  $\delta$ Orn turns. The  $\beta$ -hairpin peptide has a major surface that displays eight residues (red) and a minor surface that displays six residues (blue).

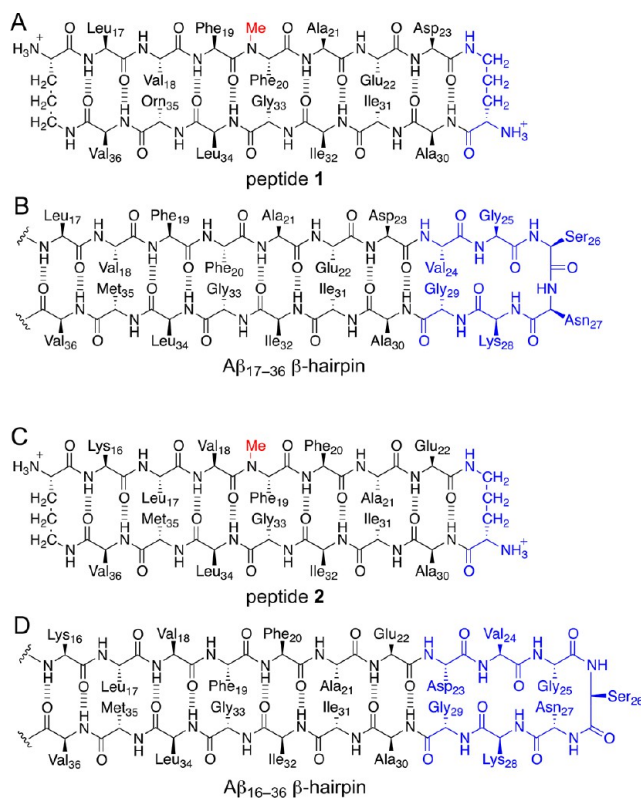


**Figure 2.** Macrocytic  $\beta$ -sheet peptides designed to mimic two different  $\beta$ -hairpin registrations of  $A\beta$ . (A) Chemical structure of peptide 1. The  $\delta$ Orn turn that connects Asp<sub>23</sub> and Ala<sub>30</sub> (blue) replaces  $A\beta_{24–29}$ . (B) Chemical structure of an  $A\beta_{17–36}$   $\beta$ -hairpin. (C) Chemical structure of peptide 2. The  $\delta$ Orn turn that connects Glu<sub>22</sub> and Ala<sub>30</sub> (blue) replaces  $A\beta_{23–29}$ . (D) Chemical structure of an  $A\beta_{16–36}$   $\beta$ -hairpin.

ray crystallography reveals that peptide 2 also assembles to form a hexamer in the crystal state. The hexamer may be considered as being composed of either dimers or trimers. The hexamer formed by peptide 2 is significant because it shares key characteristics with the oligomers formed by full-length amyloidogenic peptides and proteins and provides a structural model for an oligomer of  $A\beta$ .

## MATERIALS AND METHODS

Synthesis of peptides 1–4, SDS-PAGE, size exclusion chromatography (SEC), X-ray crystallography, lactate dehydrogenase (LDH) release assays, and replica-exchange molecular dynamics (REMD) were performed as described previously.<sup>26–30</sup> These procedures are restated in detail in the Materials and Methods in the Supporting Information.

## RESULTS AND DISCUSSION

**Oligomerization of Peptide 2.** Peptide 2 assembles to form a hexamer in SDS-PAGE. Tricine SDS-PAGE followed by silver staining shows that 1.8 kDa peptide 2 migrates just above the 10 kDa band of the ladder (Figure 4A).<sup>37</sup> The band from peptide 2 is comet-shaped and streaks downward, suggesting that the hexamer is in equilibrium with lower-molecular weight species. To further confirm the oligomerization state of peptide 2, we compared it to covalent trimer peptides 5 and 6 [Figures S1 and S2, Protein Data Bank (PDB) entries 5SUT and 5SUR, respectively], which we had previously

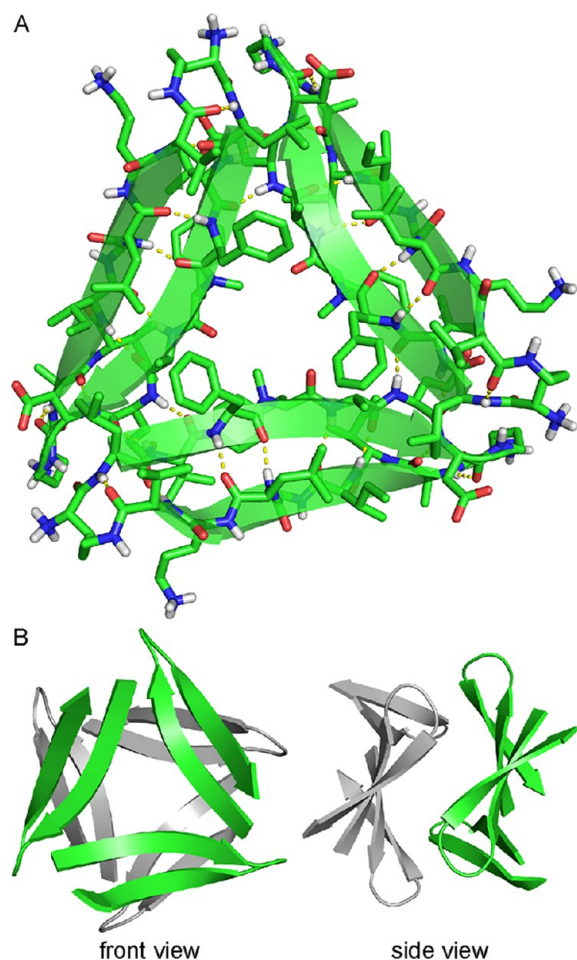


**Figure 3.** (A) X-ray crystallographic structure of the trimer formed by peptide 1 (Protein Data Bank entry 4NW9). (B) Front view and side view of the X-ray crystallographic structure of the hexamer formed by two trimers of peptide 1.

determined to migrate as 10.6 kDa hexamers and 21.2 kDa dodecamers, respectively, in equilibrium with the 5.3 kDa trimers.<sup>28</sup> Peptide 2 migrates at the same molecular weight as the hexamer band of peptide 5, providing further evidence that peptide 2 assembles to form a hexamer in SDS-PAGE. In contrast, peptide 1 does not assemble to form a hexamer in SDS-PAGE. Peptide 1 migrates well below the trimer band of peptide 6 and slightly below the 4.6 kDa band of the ladder, suggesting that peptide 1 migrates as a monomer or dimer.

Size exclusion chromatography reveals that peptide 2 also assembles to form oligomers in the absence of SDS. The elution profile of peptide 2 was compared to those of the size standards vitamin B<sub>12</sub>, aprotinin, and cytochrome *c*, as well as peptide 1. Peptide 2 elutes as a broad peak with three distinct humps (Figure 4B). The elution volumes of the humps are consistent with the molecular weights of a monomer, dimer, and trimer. The broadness of the humps suggests moderately slow exchange among the trimer, dimer, and monomer. Peptide 1 elutes as two distinct peaks: a larger peak with an elution volume consistent with the molecular weight of a dimer and a smaller peak with an elution volume consistent with the molecular weight of a trimer (Figure 4B). Table 1 summarizes the SEC data for peptides 1 and 2.

These solution-phase studies show that peptide 2 assembles to form oligomers in solution. In SDS-PAGE, peptide 2

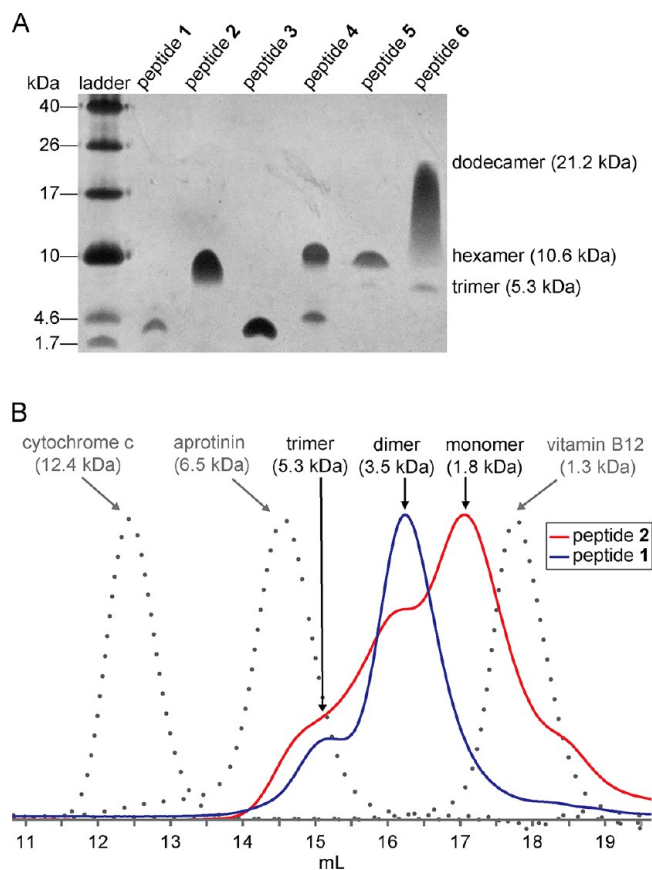


**Figure 4.** Peptide 2 assembles in solution to form oligomers. (A) Silver-stained SDS-PAGE gel. SDS-PAGE was performed on 0.15 mg/mL samples of peptides 1–4 and 0.05 mg/mL samples of peptides 5 and 6 in Tris buffer (pH 6.8) with 2% (w/v) SDS. Molecular weights calculated for the trimer, hexamer, and dodecamer are listed in parentheses. (B) SEC chromatograms. SEC was performed on a 1.0 mg/mL solution of peptide in 50 mM Tris buffer (pH 7.4) with 150 mM NaCl on a Superdex 75 10/300 column.

**Table 1.** Size Exclusion Chromatography Data for Peptides 1–4

compound	molecular weight (kDa)	elution volume (mL)	oligomer size
peptide 1	1.74	16.2, 15.1	dimer, trimer
peptide 2	1.77	17.0, 16.1, 14.8	monomer, dimer, trimer
peptide 3	1.79	17.6	monomer
peptide 4	1.72	17.0	monomer
vitamin B <sub>12</sub>	1.3	17.8	
aprotinin	6.5	14.6	
cytochrome <i>c</i>	12.4	12.4	

assembles to form a hexamer. In SEC in Tris buffer, peptide 2 assembles to form dimers and trimers. These results suggest the intriguing hypothesis that the hexamer in SDS-PAGE may be composed of dimers or trimers that further assemble to form a hexamer in the lipophilic environment of SDS micelles. We turned to X-ray crystallography to gain insights into the structures of these oligomers and thus further explore this hypothesis.

**X-ray Crystallographic Structure of Peptide 2.** Peptide 2 afforded crystals suitable for X-ray diffraction from aqueous HEPES buffer with sodium citrate and isopropanol. To

determine the X-ray crystallographic phases of peptide 2, we soaked a crystal of the peptide in potassium iodide to incorporate iodide ions into the crystal lattice and performed conventional single-wavelength anomalous diffraction (SAD) phasing.<sup>28,38,39</sup> The X-ray crystallographic structure of KI-soaked peptide 2 (PDB entry 5W4I) was then used as a search model for molecular replacement to determine the X-ray crystallographic phases of a higher-resolution data set of unsoaked peptide 2, which was collected using a synchrotron radiation source (PDB entry 5W4H).

The X-ray crystallographic structure of peptide 2 reveals that the peptide folds to form a twisted  $\beta$ -hairpin. The side chains displayed on the major and minor surfaces of peptide 2 differ from those displayed on the major and minor surfaces of peptide 1. The major surface of the peptide 2  $\beta$ -hairpin displays the side chains of Lys<sub>16</sub>, Val<sub>18</sub>, Phe<sub>20</sub>, Glu<sub>22</sub>, Ala<sub>30</sub>, Ile<sub>32</sub>, Leu<sub>34</sub>, and Val<sub>36</sub>, while the major surface of the peptide 1  $\beta$ -hairpin displays the side chains of Leu<sub>17</sub>, Phe<sub>19</sub>, Ala<sub>21</sub>, Asp<sub>23</sub>, Ala<sub>30</sub>, Ile<sub>32</sub>, Leu<sub>34</sub>, and Val<sub>36</sub> (Figure 5A). The minor surface of the peptide 2  $\beta$ -hairpin displays the side chains of Leu<sub>17</sub>, Phe<sub>19</sub>, Ala<sub>21</sub>, Ile<sub>31</sub>, Gly<sub>33</sub>, and Met<sub>35</sub>, while the minor surface of the peptide 1  $\beta$ -hairpin displays the side chains of Val<sub>18</sub>, Phe<sub>20</sub>, Glu<sub>22</sub>, Ile<sub>31</sub>, Gly<sub>33</sub>, and Orn<sub>35</sub> (Figure 5B). Thus, the minor surface of peptide 2 is wholly hydrophobic, while the minor surface of peptide 1 is not.

In the X-ray crystallographic structure of peptide 2, six  $\beta$ -hairpin monomers assemble to form a hexamer. The hexamer is composed of smaller oligomers and can be interpreted either as a trimer of dimers or as a dimer of trimers. Figure 6 shows the structure of the hexamer and illustrates these two interpretations. In Figure 6B, one dimer subunit is colored green; in Figure 6C, one trimer subunit is colored cyan. The following subsections detail the structure of the hexamer as well as the structures of the component dimers or trimers.

**Hexamer.** The hexamer formed by peptide 2 resembles a barrel with three openings (Figure 7). The interior of the barrel is filled with the side chains of residues on the minor surface of peptide 2 (Leu<sub>17</sub>, Phe<sub>19</sub>, Ala<sub>21</sub>, Ile<sub>31</sub>, Gly<sub>33</sub>, and Met<sub>35</sub>), creating a packed hydrophobic core that stabilizes the hexamer (Figure 7C). A network of hydrogen bonds between the main chains of the monomer subunits further stabilizes the hexamer. The outer

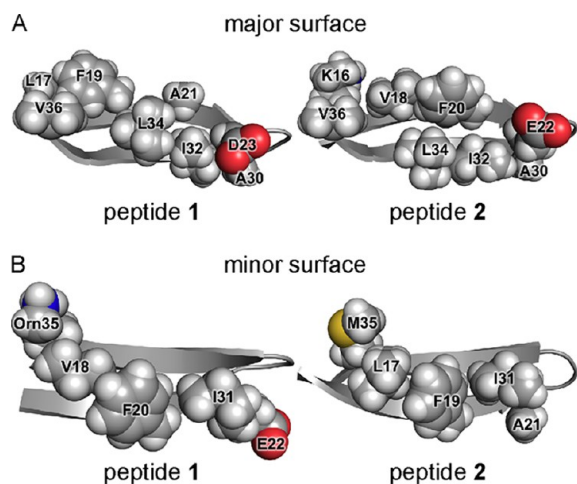


**Figure 5.** X-ray crystallographic structures of peptide 1 (PDB entry 4N9W) and peptide 2 (PDB entry 5W4H). (A) Major surfaces of peptides 1 and 2. (B) Minor surfaces of peptides 1 and 2.

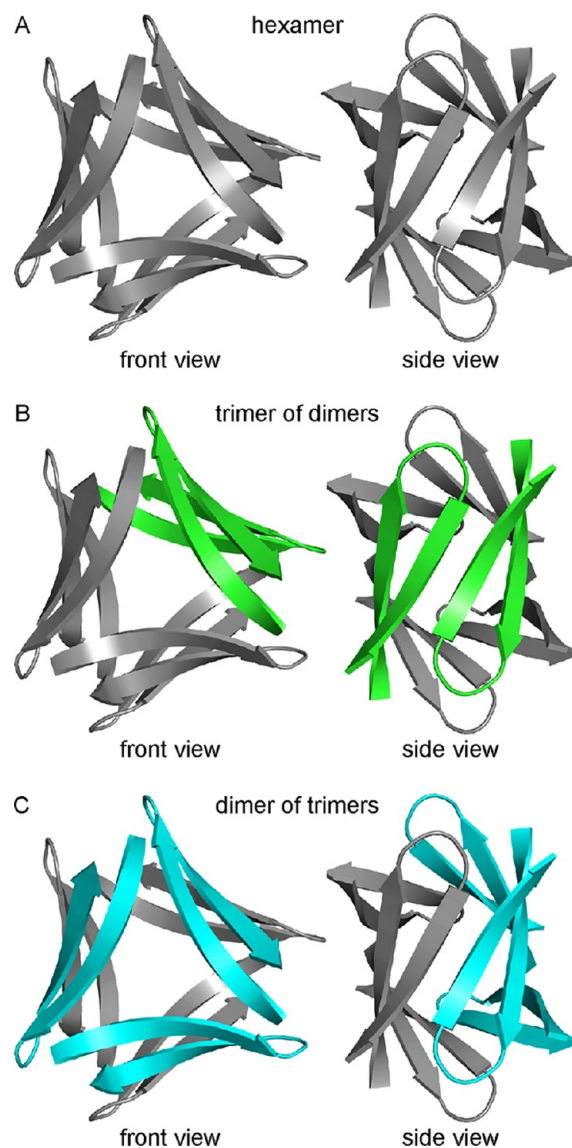


**Figure 6.** Hexamer formed by peptide 2 that can be interpreted either as a trimer of dimers or as a dimer of trimers. (A) X-ray crystallographic structure of the hexamer formed by peptide 2. (B) Interpretation of the hexamer as a trimer of dimers. One dimer subunit is colored green. (C) Interpretation of the hexamer as a dimer of trimers. One trimer subunit is colored cyan.

surface of the hexamer displays the side chains of residues on the major surface of peptide 2 (Lys<sub>16</sub>, Val<sub>18</sub>, Phe<sub>20</sub>, Glu<sub>22</sub>, Ala<sub>30</sub>, Ile<sub>32</sub>, Leu<sub>34</sub>, and Val<sub>36</sub>).

The hexamer formed by peptide 2 is more hydrogen bonded and better packed than the hexamer formed by peptide 1 (Figure S3). The hexamer formed by peptide 2 forms a continuous hydrogen-bonding network containing 30 intermolecular hydrogen bonds, whereas the hexamer formed by peptide 1 does not form a continuous hydrogen-bonding network and contains only 18 intermolecular hydrogen bonds. In the hexamer formed by peptide 1, each  $\beta$ -hairpin monomer is hydrogen bonded to only the two adjacent  $\beta$ -hairpin monomers within the triangular trimer; in the hexamer formed by peptide 2, each  $\beta$ -hairpin monomer is hydrogen bonded not only to the two adjacent monomers within the triangular trimer but also to the adjacent monomer within the  $\beta$ -sheet dimer. For these reasons, the hexamer formed by peptide 2 can be

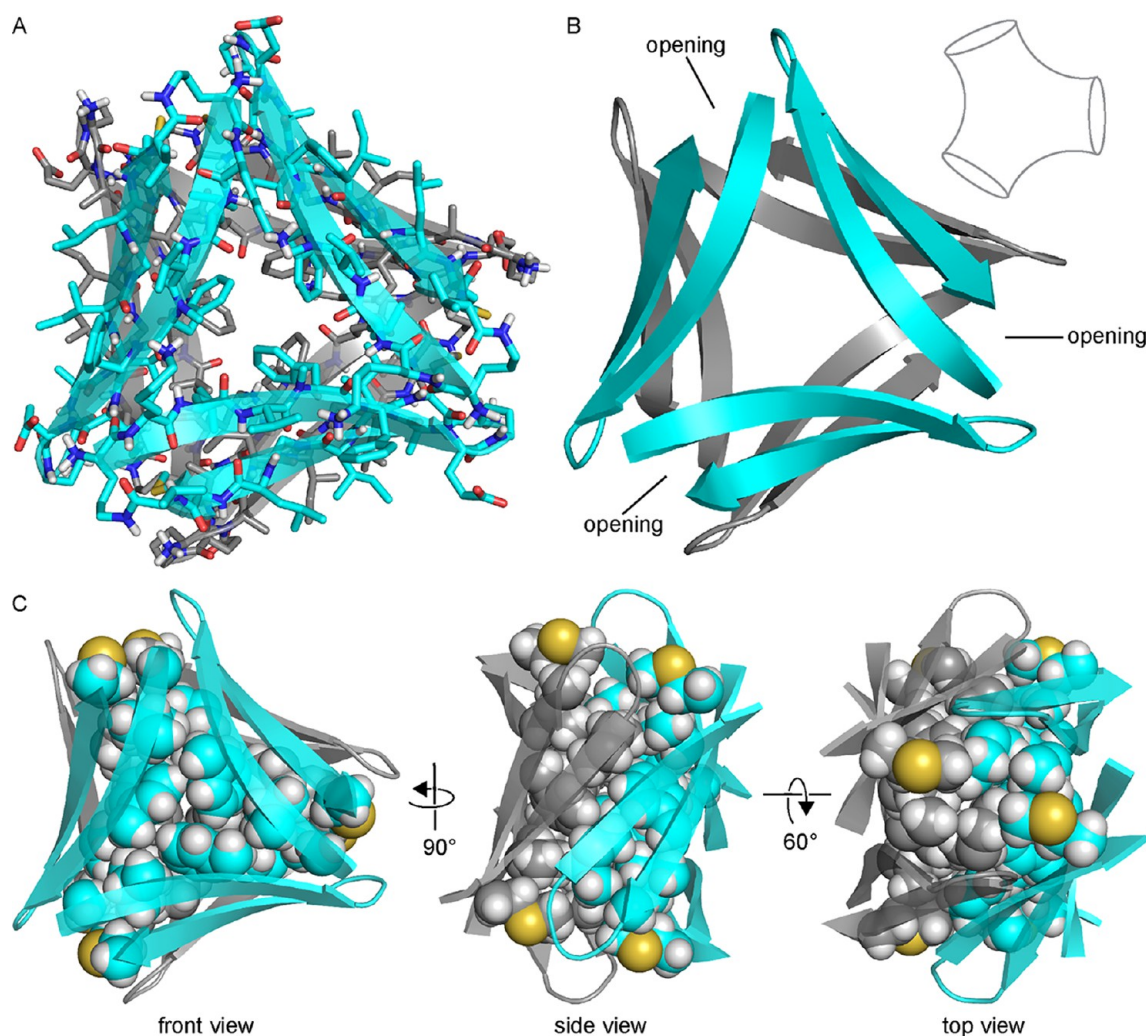


**Figure 7.** X-ray crystallographic structure of the hexamer formed by peptide 2 (PDB entry 5W4H). (A) Cartoon and stick model. (B) Cartoon model illustrating the three barrel-like openings. The inset shows a schematic representation of the general shape of the hexamer. (C) Three different views of the hexamer. Side chains of residues that pack in the hydrophobic core of the hexamer are shown as spheres. The top view looks inside one of the three barrel-like openings.

interpreted either as a trimer of  $\beta$ -sheet dimers or as a dimer of triangular trimers, whereas the hexamer formed by peptide 1 is unambiguously a dimer of triangular trimers.

Six sets of side chains from Leu<sub>17</sub>, Phe<sub>19</sub>, Ala<sub>21</sub>, Ile<sub>31</sub>, and Met<sub>35</sub> pack together to form a hydrophobic core that stabilizes the hexamer formed by peptide 2. While the minor surface of peptide 2 displays five hydrophobic side chains, that of peptide 1 displays only three (Val<sub>18</sub>, Phe<sub>20</sub>, and Ile<sub>31</sub>). The hexamer formed by peptide 1 lacks the massive hydrophobic core and is only loosely packed at the interface between trimers. The buried surface area of the hexamer formed by peptide 2 is 5102 Å<sup>2</sup>, whereas the buried surface area of the hexamer formed by peptide 1 is only 3514 Å<sup>2</sup>.

**Dimer.** Two peptide 2  $\beta$ -hairpin monomers assemble in an edge-to-edge manner to form a hydrogen-bonded dimer, creating a four-stranded antiparallel  $\beta$ -sheet (Figure 8A). (Three such dimers make up the hexamer.) The  $\beta$ -hairpin monomers are shifted out of registration by two residues toward the N-termini, such that Ala<sub>30</sub> on one monomer is across from Leu<sub>34</sub> on the adjacent monomer (Figure 8B). Four intermolecular hydrogen bonds between Ile<sub>31</sub> and Gly<sub>33</sub> of one

monomer and Gly<sub>33</sub> and Ile<sub>31</sub> of the adjacent monomer help stabilize the dimer.

The  $\beta$ -sheet dimer has two surfaces: one surface displays the side chains of residues on the major surface of peptide 2; the other surface displays the side chains of residues on the minor surface of peptide 2 (Figure 8C). Hydrophobic packing between the side chains of residues on the minor surface further stabilizes the dimer: Leu<sub>17</sub>, Phe<sub>19</sub>, and Ile<sub>31</sub> on one monomer pack against Ile<sub>31</sub>, Phe<sub>19</sub>, and Leu<sub>17</sub> on the adjacent monomer. There are no substantial intermolecular contacts between the side chains of residues on the major surface of the dimer.

**Trimer.** Three peptide 2  $\beta$ -hairpin monomers assemble to form a triangular trimer (Figure 9A). (Two such trimers make up the hexamer.) The trimer is stabilized by intermolecular edge-to-edge hydrogen bonds between monomers, which create four-stranded  $\beta$ -sheets at each corner of the trimer. At each corner, the main chain of  $\delta$ Orn of one monomer hydrogen bonds with the main chain of Ala<sub>21</sub> of the adjacent monomer, and the carbonyl of Phe<sub>19</sub> of one monomer hydrogen bonds with the NH of Leu<sub>17</sub> of the adjacent monomer (Figure 9B).

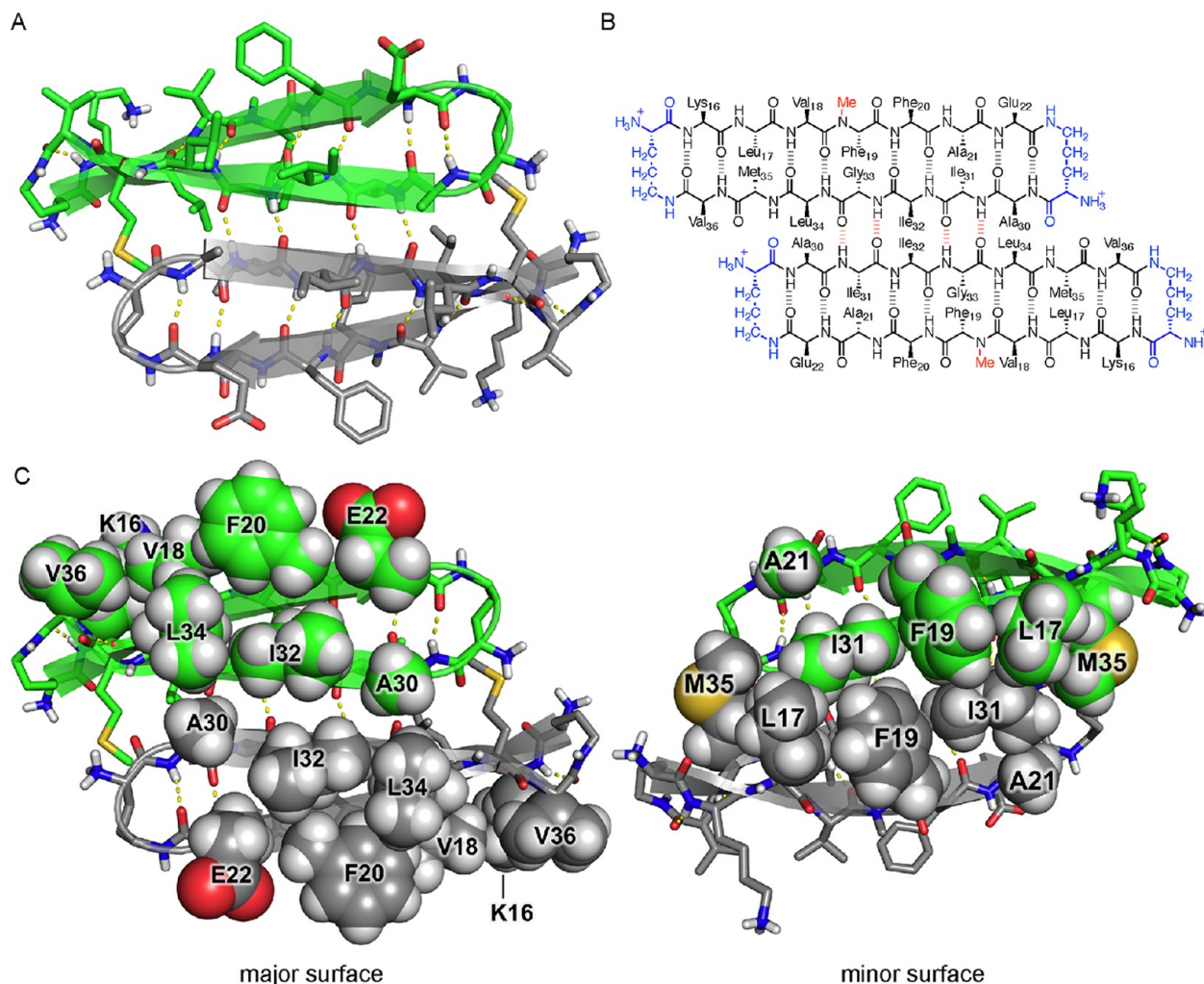


**Figure 8.**  $\beta$ -Sheet dimer formed by peptide 2. (A) X-ray crystallographic structure (PDB entry SW4H). (B) Chemical structure. The intermolecular hydrogen bonds between Ile<sub>31</sub> and Gly<sub>33</sub> are colored red. (C) View of the dimer illustrating the major and minor surfaces.

The triangular trimer has two surfaces that display the amino acid side chains of the major surfaces and the minor surfaces of the component  $\beta$ -hairpin monomers (Figure 9C). Hydrophobic packing between the side chains of residues on the minor surface further stabilizes the trimer: Met<sub>35</sub>, Leu<sub>17</sub>, and Phe<sub>19</sub> on one monomer pack against Ala<sub>21</sub>, Ile<sub>31</sub>, and Phe<sub>19</sub> on the adjacent monomer. There are no substantial intermolecular contacts between side chains of residues on the major surface of the trimer.

The hexamer, trimer, and dimer observed in the X-ray crystallographic structure of peptide 2 recapitulate the oligomers observed via SDS-PAGE and SEC. The assembly of the hexamer from either dimers or trimers may explain how the peptide 2 dimers and trimers observed in SEC come together to form the hexamer in SDS-PAGE. The structure of the hexamer shows key stabilizing contacts, such as edge-to-edge hydrogen bonding and hydrophobic packing. To better understand the importance of these contacts in the solution-phase oligomerization of peptide 2, we designed peptides 3 and 4. The following sections describe studies of these peptides and also provide insights into why A $\beta$ <sub>16–36</sub>-derived peptide 2 forms a hexamer in SDS-PAGE but A $\beta$ <sub>17–36</sub>-derived peptide 1 does not.

**N-Methylation of Peptide 2 Disrupts Oligomerization.** To test whether the hexamer observed in SDS-PAGE is similar

in structure to the hexamer observed crystallographically, we prepared a homologue containing an additional *N*-methyl group designed to disrupt hexamer formation. Peptide 3 is a homologue of peptide 2 bearing an additional *N*-methyl group on Gly<sub>33</sub> (Figure 10A). In the X-ray crystallographic structure of the hexamer formed by peptide 2, the backbone of Gly<sub>33</sub> on one monomer hydrogen bonds with the backbone of Ile<sub>31</sub> on an adjacent monomer (Figure 8B). Introduction of an *N*-methyl group on Gly<sub>33</sub> should prevent hydrogen bonding and thus disrupt the hexamer. In SDS-PAGE, peptide 3 does not migrate as a hexamer (Figure 4A). Instead, peptide 3 migrates like peptide 1 and thus appears to run as a monomer or dimer. This result supports a model in which the hexamer formed by peptide 2 in SDS-PAGE is similar in structure to the hexamer observed crystallographically. In SEC, peptide 3 elutes at a volume consistent with the molecular weight of a monomer (Table 1), further demonstrating that *N*-methylation on Gly<sub>33</sub> disrupts oligomer formation.

**Mutation of Peptide 1 Induces Oligomerization.** The SDS-PAGE and X-ray crystallographic studies of peptides 1 and 2 demonstrate that shifting the registration of a  $\beta$ -hairpin peptide affects its oligomerization. In the X-ray crystallographic structures, the hexamer formed by peptide 2 is better packed and has more hydrogen bonds than the hexamer formed by peptide 1. In SDS-PAGE, peptide 2 assembles to form a

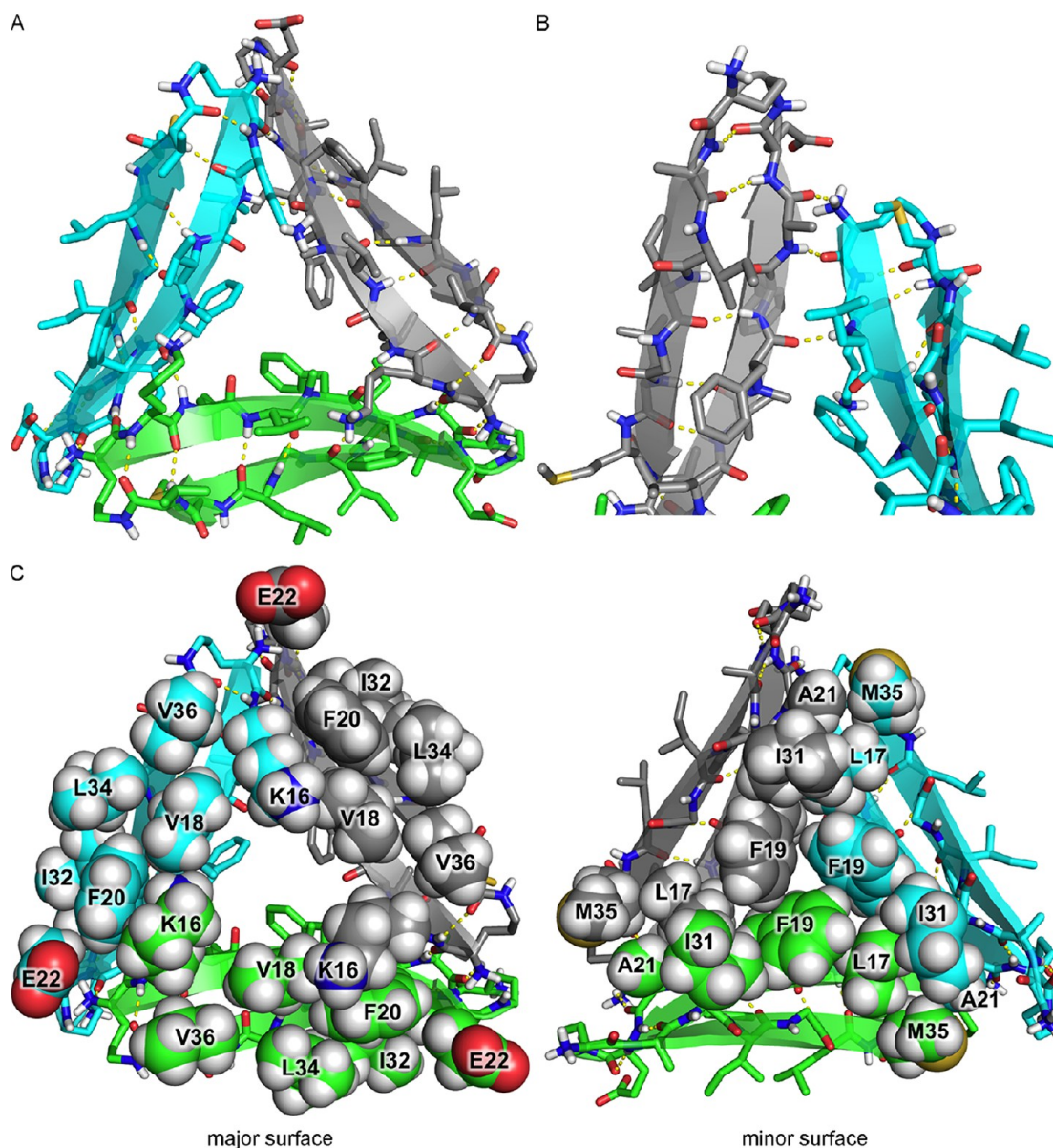


**Figure 9.** X-ray crystallographic structure of the trimer formed by peptide 2 (PDB entry SW4H). (A) Cartoon and stick model. (B) Detailed view of a corner of the triangular trimer showing the intermolecular hydrogen bonding between monomers, which creates a four-stranded  $\beta$ -sheet. (C) View of the trimer illustrating the major and minor surfaces.

hexamer, whereas peptide 1 does not. The difference in the hydrophobicity and charge of the minor surfaces of peptides 1 and 2 may explain this difference in oligomerization. The minor surface of peptide 1 displays two charged hydrophilic side chains and three hydrophobic side chains, whereas the minor surface of peptide 2 displays five hydrophobic side chains (Figure 11).

To explore the importance of charge and hydrophobicity in oligomerization, we prepared peptide 4 (Figure 10B). Peptide 4 is a triple mutant of peptide 1, with L17K, E22A, and Orn35M mutations. Peptide 4 may be considered as a chimera in which three residues of peptide 2 are grafted onto peptide 1 to eliminate charge on the minor surface. In peptide 4, Ala<sub>22</sub> and Met<sub>35</sub> occupy the same sites on the minor surface as Ala<sub>21</sub> and Met<sub>35</sub> in peptide 2. The Lys<sub>17</sub> residue in peptide 4 sits on the major surface, occupying the same site as Lys<sub>16</sub> in peptide 2 and providing charge to enhance solubility. The 11 remaining residues of peptide 4 are identical to those of peptide 1.

SDS–PAGE reveals that peptide 4 assembles to form an oligomer that migrates at a molecular weight slightly higher than that of the hexamer formed by peptide 2 (Figure 4A). Replacement of the charged residues with hydrophobic residues on the minor surface of peptide 1 converts a peptide that does not form oligomers in aqueous SDS to a peptide that oligomerizes. This experiment confirms the importance of an uncharged, hydrophobic surface in the oligomerization of  $\beta$ -hairpin peptides. In SEC, peptide 4 elutes at a volume consistent with the molecular weight of a monomer (Table 1), suggesting that SDS promotes oligomerization of peptide 4 in the SDS–PAGE experiment.

The slightly higher position of the peptide 4 oligomer band in SDS–PAGE suggests that the oligomer formed by peptide 4 may differ in structure from the hexamer formed by peptide 2. To gain insights into the structure of the oligomer formed by peptide 4, we turned to X-ray crystallography. Peptide 4 afforded crystals suitable for X-ray diffraction in aqueous

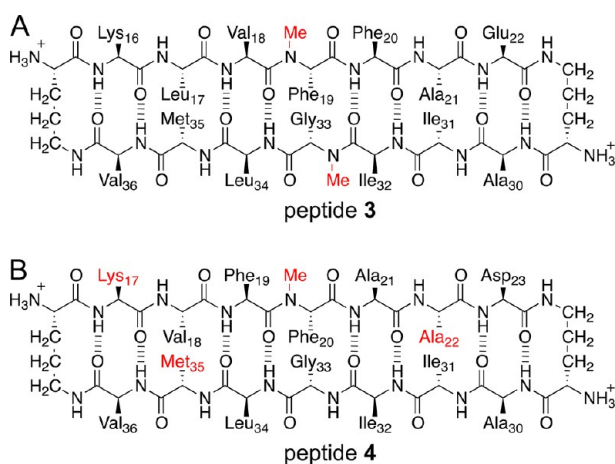


**Figure 10.** (A) Chemical structure of peptide 3, a homologue of peptide 2 bearing an additional *N*-methyl group. (B) Chemical structure of peptide 4, a triple mutant of peptide 1. The mutated residues are colored red.

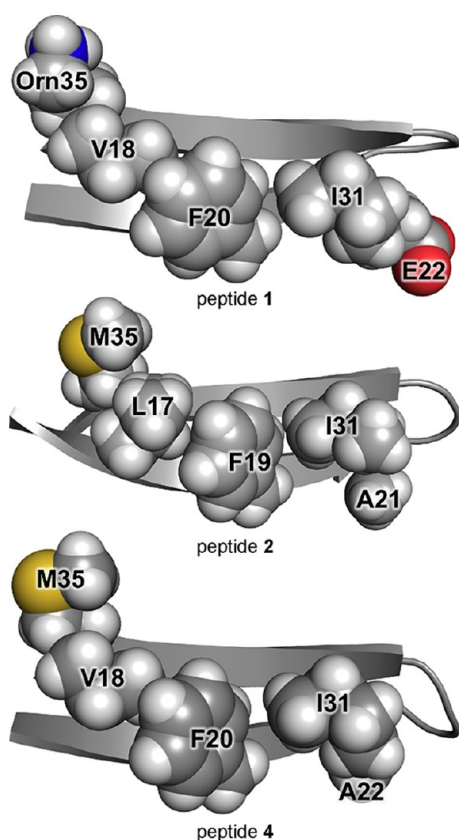


**Figure 11.** X-ray crystallographic structures of peptides 1, 2, and 4, highlighting the minor surfaces of the peptides (PDB entries 4NW9, 5W4H, and 5W4J, respectively).

HEPES buffer with potassium chloride and pentaerythritol propoxylate. We determined the X-ray crystallographic phases of peptide 4 by sulfur single-wavelength anomalous diffraction (S-SAD) using the anomalous signal from the sulfur in methionine.<sup>40,41</sup>

X-ray crystallography reveals that peptide 4 folds to form  $\beta$ -hairpins similar to those formed by peptides 1 and 2 (Figure 11). The minor surface of peptide 4 is nearly identical to that of peptide 2, except that Val<sub>18</sub> takes the place of Leu<sub>17</sub>. Peptide 4

assembles differently than peptides 1 and 2, forming packed columns in the crystal lattice rather than discrete oligomers (Figure 12B). The columns are composed of antiparallel  $\beta$ -sheet dimers that are laminated on both faces through hydrophobic interactions. Each dimer consists of an antiparallel  $\beta$ -sheet formed by two peptide 4  $\beta$ -hairpins (Figure 12A). The dimer is shifted out of registration by two residues toward the C-termini, such that Met<sub>35</sub> pairs with Gly<sub>33</sub>. The oligomer formed by peptide 4 in SDS-PAGE might be composed of three or four of these dimers packing through hydrophobic interactions.

**Biological Studies of Peptides 1–4.** Many oligomers formed by full-length *A $\beta$*  are toxic toward cells.<sup>7,8</sup> To test whether the oligomers formed by peptide 2 are also toxic, we evaluated the toxicity of peptide 2 toward neuronally derived SH-SY5Y cells using a LDH release assay. We compared peptide 2 to peptide 3 to investigate how the hexamer-forming

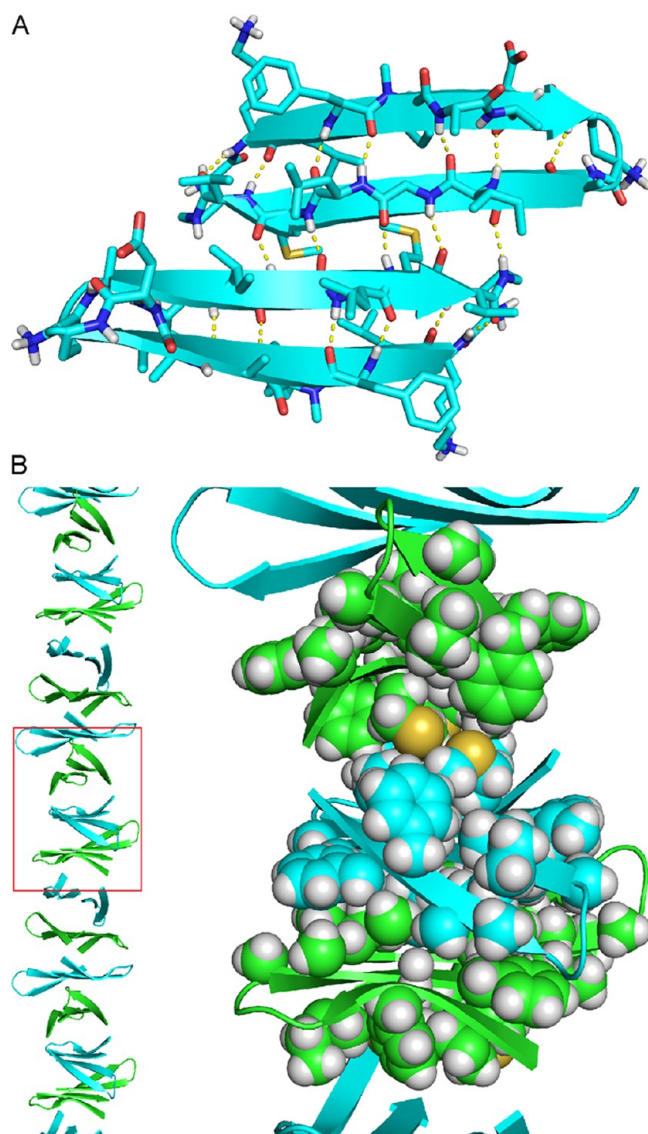


**Figure 12.** X-ray crystallographic structure of peptide 4 (PDB entry 5W4J). (A) Structure of the antiparallel  $\beta$ -sheet dimer formed by peptide 4. (B) Column of laminated antiparallel  $\beta$ -sheet dimers. The right panel shows a detailed view of the hydrophobic packing that occurs at the interfaces of the dimers.



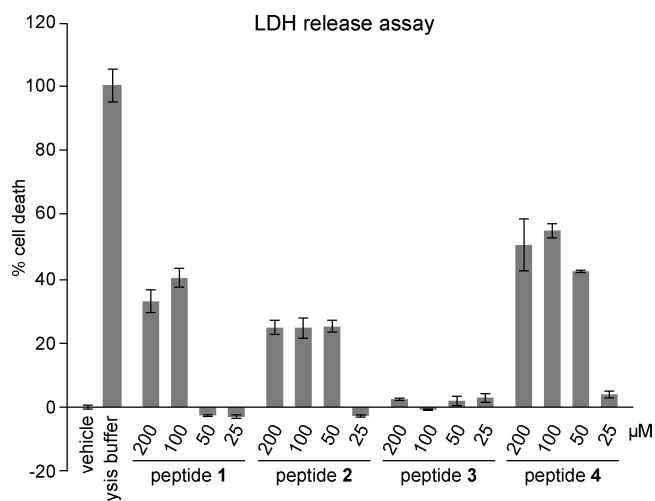


**Figure 13.** LDH release assay of peptides 1–4. Data represent the mean of five replicate wells  $\pm$  the standard deviation. Deionized water (vehicle) was used as a negative control.

$A\beta_{16-36}$ -derived peptide compares to a non-oligomerizing homologue. We also evaluated the toxicity of peptides 1 and 4 to better understand the relationship between oligomerization and toxicity.

Peptide 2 shows an increase in LDH release at concentrations as low as 50  $\mu\text{M}$ , indicating toxicity toward SH-SY5Y cells (Figure 13). Peptide 3, the non-oligomerizing homologue of peptide 2, is not toxic toward SH-SY5Y cells at concentrations as high as 200  $\mu\text{M}$ , suggesting that oligomerization of peptide 2 to form a hexamer is important for toxicity. No dose dependence is observed in the LDH release induced by peptide 2 at concentrations of 50, 100, and 200  $\mu\text{M}$ , suggesting that oligomerization is cooperative and toxicity occurs above a critical concentration. Peptide 1 is toxic toward SH-SY5Y cells at concentrations as low as 100  $\mu\text{M}$ , and peptide 4 is toxic toward SH-SY5Y cells at concentrations as low as 50  $\mu\text{M}$ .

We envision that the onset of toxicity of peptides 1, 2, and 4 between 25 and 100  $\mu\text{M}$  reflects the propensity of the hydrophobic peptides to form oligomers in the presence of the lipophilic cell membranes. In this model, none of the peptides are oligomeric in cell membranes at 25  $\mu\text{M}$ . As the

concentration is increased, oligomerization occurs, the oligomers disrupt the integrity of the cell membranes, and cell damage or death occurs.

**Crystallographically Based Model of an  $A\beta_{12-40}$  Hexamer.** We envision that the full-length  $A\beta$  peptide can assemble in the same fashion as peptide 2 to form a barrel-like hexamer composed of  $\beta$ -sheet dimers or triangular trimers. To better understand what a hexamer containing the  $A\beta_{23-29}$  loop and additional N- and C-terminal residues might look like, we modeled  $A\beta_{12-40}$  into the crystallographic coordinates of the hexamer. We built residues 23–29 (DVGSNKG), 12–15 (VHHQ), and 37–40 (GGVV) into the crystallographic coordinates of the six peptide 2 monomers that comprise the hexamer, and we performed REMD to generate realistic conformations of the loops and the N- and C-terminal regions of the  $\beta$ -hairpins (Figure 14).<sup>42,43</sup>

The REMD simulation shows that full-length  $A\beta$  could form a barrel-like hexamer. The hexamer can accommodate the  $A\beta_{23-29}$  loop and the remaining N- and C-terminal residues without steric clashes. In a hexamer formed by full-length  $A\beta$ , the loops from two monomers and the N- and C-termini from two other monomers would extend past the barrel-like openings. The loops might fold over the barrel-like openings and shield the hydrophobic core of the hexamer, which would otherwise be exposed to solvent.

## ■ SUMMARY AND CONCLUSION

These X-ray crystallographic, biophysical, and biological studies of  $\beta$ -hairpins derived from  $A\beta$  provide insights into amyloid oligomers. X-ray crystallography revealed that  $\beta$ -hairpin peptide 2 assembles to form a hexamer composed of dimers and trimers. SDS-PAGE and SEC revealed that peptide 2 assembles to form oligomers in solution that recapitulate the oligomers observed crystallographically. In the SDS-PAGE experiment, peptide 2 assembles to form a hexamer, which recapitulates the barrel-like hexamer observed crystallographically. In the SEC experiment, peptide 2 assembles to form a dimer and trimer, which recapitulate the  $\beta$ -sheet dimer and triangular trimer observed crystallographically. The difference between the assemblies observed in the SEC and SDS-PAGE experiments may be explained by the membranelike environment of SDS micelles, which appears to promote the assembly of the dimers and trimers into the hexamer.

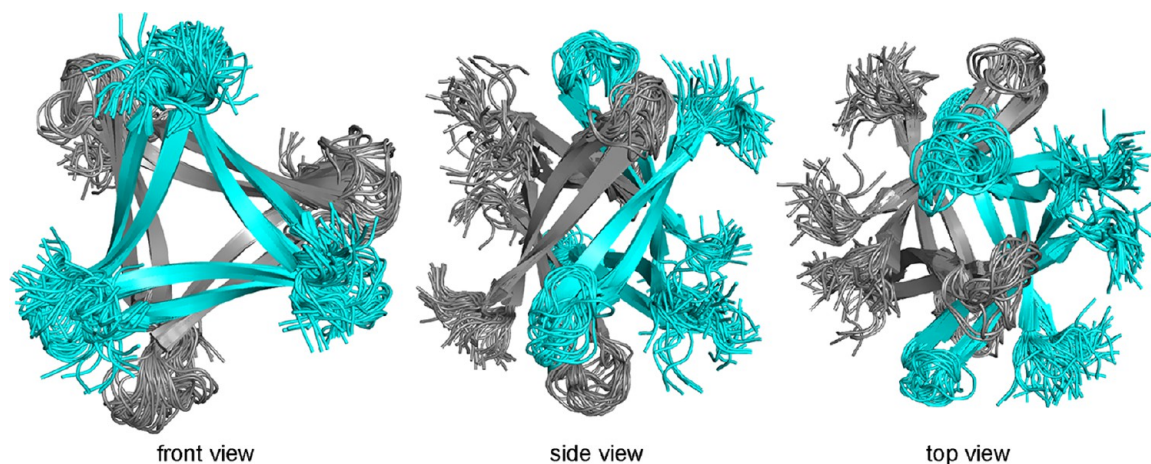


**Figure 14.** Crystallographically based model of an  $A\beta_{12-40}$  barrel-like hexamer. Superposition of 31 structures generated by REMD.

The differing propensities of peptides 1 and 2 to oligomerize in SDS–PAGE may result from differences in hydrophobicity and charge on the minor surfaces of each peptide. The oligomerization of chimera peptide 4 in SDS–PAGE supports the importance of a hydrophobic minor surface in solution-phase assembly. We recently demonstrated that stabilizing the trimer formed by peptide 1 through covalent cross-linking allows solution-phase assembly to form higher-order oligomers, such as hexamers and dodecamers.<sup>28</sup> The study presented here demonstrates that hydrophobic interactions between monomers that are not covalently cross-linked can stabilize higher-order oligomers in the same fashion. This finding is significant, because it shows that suitably folded  $\beta$ -hairpin peptides containing amyloidogenic sequences can form stable oligomers.

The X-ray crystallographic structure of the hexamer formed by peptide 2 shares structural features with the  $\alpha$ B crystallin cylindrin oligomer reported by Eisenberg and co-workers<sup>1</sup> and the hPrP oligomer reported by Surewicz and co-workers.<sup>2</sup> Like these oligomers, the hexamer formed by peptide 2 is a discrete oligomer composed of antiparallel  $\beta$ -sheets that form a continuous hydrogen-bonding network and a hydrophobic core. These features have emerged as common structural motifs among oligomers formed by amyloidogenic peptides and proteins. We have also seen this motif in a barrel-like hexamer formed by a  $\beta$ -hairpin peptide derived from  $\beta_2$ -microglobulin that assembles in a fashion similar to that of the hexamer formed by peptide 2.<sup>30</sup>

Hexamers of A $\beta$  have been isolated from the brains of Tg2576 transgenic mice as well as from human brains and are thought to play a role in the early stages of Alzheimer's disease.<sup>9,44</sup> The barrel-like hexamer formed by peptide 2 exhibits many of the biological and solution-phase characteristics of oligomers formed by full-length A $\beta$ . Like A $\beta$  oligomers, the hexamer assembles in the presence of SDS and is toxic toward cells. Despite these similarities, the significance of the barrel-like hexamer in Alzheimer's disease remains to be determined and is a current area of investigation in our laboratory.

## ■ ASSOCIATED CONTENT

### ■ Supporting Information

The Supporting Information is available free of charge on the ACS Publications website at DOI: 10.1021/acs.biochem.7b00831.

Procedures for the synthesis of peptides 1–4, crystallization of peptides 2 and 4, SDS–PAGE and silver staining, size exclusion chromatography, and LDH release assays; characterization data for peptides 1–4; and details of X-ray crystallographic data collection, processing, and refinement (PDF)  
Data for PDB entry 5W4H (CIF)  
Data for PDB entry 5W4I (CIF)  
Data for PDB entry 5W4J (CIF)

### Accession Codes

Crystallographic coordinates of peptide 2 were deposited in the PDB as entries 5W4H (data collected on a synchrotron at a wavelength of 0.998 Å) and 5W4I (data collected on an X-ray diffractometer at a wavelength of 1.54 Å). Crystallographic coordinates of peptide 4 were also deposited in the PDB as entry 5W4J.

## ■ AUTHOR INFORMATION

### Corresponding Author

\*E-mail: jsnowick@uci.edu.

### ORCID

Ryan K. Spencer: 0000-0002-1043-3913

James S. Nowick: 0000-0002-2273-1029

### Funding

Supported by the National Institutes of Health's National Institute of General Medical Sciences via Grant GM097562.

### Notes

The authors declare no competing financial interest.

## ■ ACKNOWLEDGMENTS

The authors thank Dr. Huiying Li for helpful advice and assistance and the Berkeley Center for Structural Biology (BCSB) of the Advanced Light Source (ALS) for synchrotron data collection. The BCSB is supported in part by the National Institute of General Medical Sciences and the Howard Hughes Medical Institute. The ALS is supported by the Director, Office of Science, Office of Basic Energy Sciences, of the U.S. Department of Energy under Contract DE-AC02-05CH11231.

## ■ REFERENCES

- (1) Laganowsky, A., Liu, C., Sawaya, M. R., Whitelegge, J. P., Park, J., Zhao, M., Pensalfini, A., Soriaga, A. B., Landau, M., Teng, P. K., Cascio, D., Glabe, C., and Eisenberg, D. (2012) Atomic view of a toxic amyloid small oligomer. *Science* 335, 1228–1231.
- (2) Apostol, M. I., Perry, K., and Surewicz, W. K. (2013) Crystal structure of a human prion protein fragment reveals a motif for oligomer formation. *J. Am. Chem. Soc.* 135, 10202–10205.
- (3) Liu, C., Sawaya, M. R., Cheng, P. N., Zheng, J., Nowick, J. S., and Eisenberg, D. (2011) Out-of-register  $\beta$ -sheets suggest a pathway to toxic amyloid aggregates. *J. Am. Chem. Soc.* 133, 6736–6744.
- (4) Pham, J. D., Chim, N., Goulding, C. W., and Nowick, J. S. (2013) Structures of oligomers of a peptide from  $\beta$ -amyloid. *J. Am. Chem. Soc.* 135, 12460–12467.
- (5) Kaye, R., Head, E., Thompson, J. L., McIntire, T. M., Milton, S. C., Cotman, C. W., and Glabe, C. G. (2003) Common structure of soluble amyloid oligomers implies common mechanism of pathogenesis. *Science* 300, 486–489.
- (6) Glabe, C. G. (2008) Structural classification of toxic amyloid oligomers. *J. Biol. Chem.* 283, 29639–29643.
- (7) Benilova, I., Karran, E., and De Strooper, B. (2012) The toxic A $\beta$  oligomer and Alzheimer's disease: an emperor in need of clothes. *Nat. Neurosci.* 15, 349–357.
- (8) Larson, M. E., and Lesné, S. E. (2012) Soluble A $\beta$  oligomer production and toxicity. *J. Neurochem.* 120, 125–139.
- (9) Lesné, S., Koh, M. T., Kotilinek, L., Kaye, R., Glabe, C. G., Yang, A., Gallagher, M., and Ashe, K. H. (2006) A specific amyloid-beta protein assembly in the brain impairs memory. *Nature* 440, 352–357.
- (10) Shankar, G. M., Li, S., Mehta, T. H., Garcia-Munoz, A., Shepardson, N. E., Smith, I., Brett, F. M., Farrell, M. A., Rowan, M. J., Lemere, C. A., Regan, C. M., Walsh, D. M., Sabatini, B. L., and Selkoe, D. J. (2008) Amyloid-beta protein dimers isolated directly from Alzheimer's brains impair synaptic plasticity and memory. *Nat. Med.* 14, 837–842.
- (11) Wälti, M. A., Ravotti, F., Arai, H., Glabe, C. G., Wall, J. S., Böckmann, A., Güntert, P., Meier, B. H., and Riek, R. (2016) Atomic-resolution structure of a disease-relevant A $\beta$ (1–42) amyloid fibril. *Proc. Natl. Acad. Sci. U. S. A.* 113, E4976–E4984.
- (12) Colvin, M. T., Silvers, R., Ni, Q. Z., Can, T. V., Sergeyev, I., Rosay, M., Donovan, K. J., Michael, B., Wall, J., Linse, S., and Griffin, R. G. (2016) Atomic Resolution Structure of Monomeric A $\beta$ 42 Amyloid Fibrils. *J. Am. Chem. Soc.* 138, 9663–9674.

- (13) Lu, J. X., Qiang, W., Yau, W. M., Schwieters, C. D., Meredith, S. C., and Tycko, R. (2013) Molecular structure of  $\beta$ -amyloid fibrils in Alzheimer's disease brain tissue. *Cell* 154, 1257–1268.
- (14) Tuttle, M. D., Comellas, G., Nieuwkoop, A. J., Covell, D. J., Berthold, D. A., Kloepper, K. D., Courtney, J. M., Kim, J. K., Barclay, A. M., Kendall, A., Wan, W., Stubbs, G., Schwieters, C. D., Lee, V. M., George, J. M., and Rienstra, C. M. (2016) Solid-state NMR structure of a pathogenic fibril of full-length human  $\alpha$ -synuclein. *Nat. Struct. Mol. Biol.* 23, 409–415.
- (15) Gu, L., Liu, C., and Guo, Z. (2013) Structural insights into A $\beta$ 42 oligomers using site-directed spin labeling. *J. Biol. Chem.* 288, 18673–18683.
- (16) Potapov, A., Yau, W.-M., Ghirlando, R., Thurber, K. R., and Tycko, R. (2015) Successive Stages of Amyloid- $\beta$  Self-Assembly Characterized by Solid-State Nuclear Magnetic Resonance with Dynamic Nuclear Polarization. *J. Am. Chem. Soc.* 137, 8294–8307.
- (17) Hoyer, W., Grönwall, C., Jonsson, A., Ståhl, S., and Härd, T. (2008) Stabilization of a beta-hairpin in monomeric Alzheimer's amyloid-beta peptide inhibits amyloid formation. *Proc. Natl. Acad. Sci. U. S. A.* 105, 5099–6104.
- (18) Sandberg, A., Luheshi, L. M., Söllvander, S., Pereira de Barros, T., Macao, B., Knowles, T. P., Biverstål, H., Lendel, C., Ekholm-Peterson, F., Dubnovitsky, A., Lannfelt, L., Dobson, C. M., and Härd, T. (2010) Stabilization of neurotoxic Alzheimer amyloid-beta oligomers by protein engineering. *Proc. Natl. Acad. Sci. U. S. A.* 107, 15595–15600.
- (19) Lendel, C., Bjerring, M., Dubnovitsky, A., Kelly, R. T., Filippov, A., Antzutkin, O. N., Nielsen, N. C., and Härd, T. (2014) A hexameric peptide barrel as building block of amyloid- $\beta$  protofibrils. *Angew. Chem., Int. Ed.* 53, 12756–12760.
- (20) Mirecka, E. A., Shaykhalshahi, H., Gauhar, A., Akgül, Ş., Lecher, J., Willbold, D., Stoldt, M., and Hoyer, W. (2014) Sequestration of a  $\beta$ -hairpin for control of  $\alpha$ -synuclein aggregation. *Angew. Chem., Int. Ed.* 53, 4227–4230.
- (21) Mirecka, E. A., Feuerstein, S., Gremer, L., Schröder, G. F., Stoldt, M., Willbold, D., and Hoyer, W. (2016)  $\beta$ -Hairpin of Islet Amyloid Polypeptide Bound to an Aggregation Inhibitor. *Sci. Rep.* 6, 33474.
- (22) Yu, L., Edalji, R., Harlan, J. E., Holzman, T. F., Lopez, A. P., Labkovsky, B., Hillen, H., Barghorn, S., Ebert, U., Richardson, P. L., Miesbauer, L., Solomon, L., Bartley, D., Walter, K., Johnson, R. W., Hajduk, P. J., and Olejniczak, E. T. (2009) Structural characterization of a soluble amyloid beta-peptide oligomer. *Biochemistry* 48, 1870–1877.
- (23) Scheidt, H. A., Morgado, I., and Huster, D. (2012) Solid-state NMR reveals a close structural relationship between amyloid- $\beta$  protofibrils and oligomers. *J. Biol. Chem.* 287, 22822–22826.
- (24) Doi, T., Masuda, Y., Irie, K., Akagi, K., Monobe, Y., Imazawa, T., and Takegoshi, K. (2012) Solid-state NMR analysis of the  $\beta$ -strand orientation of the protofibrils of amyloid  $\beta$ -protein. *Biochem. Biophys. Res. Commun.* 428, 458–462.
- (25) Tay, W. M., Huang, D., Rosenberry, T. L., and Paravastu, A. K. (2013) The Alzheimer's amyloid- $\beta$ (1–42) peptide forms off-pathway oligomers and fibrils that are distinguished structurally by intermolecular organization. *J. Mol. Biol.* 425, 2494–2508.
- (26) Spencer, R. K., Li, H., and Nowick, J. S. (2014) X-ray crystallographic structures of trimers and higher-order oligomeric assemblies of a peptide derived from A $\beta$ (17–36). *J. Am. Chem. Soc.* 136, 5595–5598.
- (27) Kreutzer, A. G., Hamza, I. H., Spencer, R. K., and Nowick, J. S. (2016) X-ray Crystallographic Structures of a Trimer, Dodecamer, and Annular Pore Formed by an A $\beta$ 17–36  $\beta$ -Hairpin. *J. Am. Chem. Soc.* 138, 4634–4642.
- (28) Kreutzer, A. G., Yoo, S., Spencer, R. K., and Nowick, J. S. (2017) Stabilization, Assembly, and Toxicity of Trimers Derived from A $\beta$ . *J. Am. Chem. Soc.* 139, 966–975.
- (29) Salveson, P. J., Spencer, R. K., and Nowick, J. S. (2016) X-ray Crystallographic Structure of Oligomers Formed by a Toxic  $\beta$ -Hairpin Derived from  $\alpha$ -Synuclein: Trimers and Higher-Order Oligomers. *J. Am. Chem. Soc.* 138, 4458–4467.
- (30) Spencer, R. K., Kreutzer, A. G., Salveson, P. J., Li, H., and Nowick, J. S. (2015) X-ray Crystallographic Structures of Oligomers of Peptides Derived from  $\beta$ 2-Microglobulin. *J. Am. Chem. Soc.* 137, 6304–6311.
- (31) Spencer, R. K., Chen, K. H., Manuel, G., and Nowick, J. S. (2013) Recipe for  $\beta$ -Sheets: Foldamers Containing Amyloidogenic Peptide Sequences. *Eur. J. Org. Chem.* 2013, 3523–3528.
- (32) Nowick, J. S., and Brower, J. O. (2003) A new turn structure for the formation of beta-hairpins in peptides. *J. Am. Chem. Soc.* 125, 876–877.
- (33) Woods, R. J., Brower, J. O., Castellanos, E., Hashemzadeh, M., Khakshoor, O., Russu, W. A., and Nowick, J. S. (2007) Cyclic modular beta-sheets. *J. Am. Chem. Soc.* 129, 2548–2558.
- (34) A homologue of peptide 2 in which the N-methyl group is on Gly<sub>33</sub> and Phe<sub>19</sub> is mutated to p-iodophenylalanine assembles to form a ball-shaped dodecamer. The placement of the N-methyl group prevents the formation of a hexamer homologous to that formed by peptide 2: Salveson, P. J., Spencer, R. K., Kreutzer, A. G., and Nowick, J. S. (2017) X-ray Crystallographic Structure of a Compact Dodecamer from a Peptide Derived from A $\beta$ 16–36. *Org. Lett.* 19, 3462–3465.
- (35) The A $\beta$ <sub>17–36</sub>  $\beta$ -hairpin embodied in peptide 1 has the same alignment of residues as the antibody-bound A $\beta$   $\beta$ -hairpin reported in ref 17.
- (36) In the X-ray crystallographic structure of peptide 1, the triangular trimer also assembles to form a ball-shaped dodecamer.
- (37) Peptide 2 was synthesized as described previously by our laboratory.<sup>26–30</sup> The peptide was synthesized by solid-phase peptide synthesis on 2-chlorotrityl resin, followed by cleavage from the resin, solution-phase cyclization, global deprotection, and purification by reverse-phase high-performance liquid chromatography.
- (38) Dauter, Z., Dauter, M., and Rajashankar, K. R. (2000) Novel approach to phasing proteins: derivatization by short cryo-soaking with halides. *Acta Crystallogr., Sect. D: Biol. Crystallogr.* 56, 232–237.
- (39) Spencer, R. K., and Nowick, J. S. (2015) A Newcomer's Guide to Peptide Crystallography. *Isr. J. Chem.* 55, 698–710.
- (40) Liu, Q., Dahmane, T., Zhang, Z., Assur, Z., Brasch, J., Shapiro, L., Mancina, F., and Hendrickson, W. A. (2012) Structures from anomalous diffraction of native biological macromolecules. *Science* 336, 1033–1037.
- (41) Sarma, G. N., and Karplus, P. A. (2006) In-house sulfur SAD phasing: a case study of the effects of data quality and resolution cutoffs. *Acta Crystallogr., Sect. D: Biol. Crystallogr.* 62, 707–716.
- (42) Sugita, Y., and Okamoto, Y. (1999) Replica-exchange molecular dynamics method for protein folding. *Chem. Phys. Lett.* 314, 141–151.
- (43) Phillips, J. C., Braun, R., Wang, W., Gumbart, J., Tajkhorshid, E., Villa, E., Chipot, C., Skeel, R. D., Kale, L., and Schulten, K. (2005) Scalable molecular dynamics with NAMD. *J. Comput. Chem.* 26, 1781–1802.
- (44) Lesné, S. E., Sherman, M. A., Grant, M., Kuskowski, M., Schneider, J. A., Bennett, D. A., and Ashe, K. H. (2013) Brain amyloid- $\beta$  oligomers in ageing and Alzheimer's disease. *Brain* 136, 1383–1398.